Pis'ma v ZhETF, vol. 91, iss. 11, pp. 669 – 675 © 2010 June 10

Orbital glass and spin glass states of ^{3}He-A in aerogel

V. V. Dmitriev, D. A. Krasnikhin, N. Mulders[+], *A. A. Senin, G. E. Volovik*[*Δ], *A. N. Yudin*

P.L. Kapitza Institute for Physical Problems RAS, 119334 Moscow, Russia

[+]*Department of Physics and Astronomy, University of Delaware, Newark, 19716 Delaware, USA*

[*]*Low Temperature Laboratory, Aalto University, FI-00076 AALTO, Finland*

[Δ]*L.D. Landau Institute for Theoretical Physics, 119334 Moscow, Russia*

Submitted 29 April 2010

Glass states of superfluid A-like phase of ^{3}He in aerogel induced by random orientations of aerogel strands are investigated theoretically and experimentally. In anisotropic aerogel with stretching deformation two glass phases are observed. Both phases represent the anisotropic glass of the orbital ferromagnetic vector $\hat{\mathbf{l}}$ – the orbital glass (OG). The phases differ by the spin structure: the spin nematic vector $\hat{\mathbf{d}}$ can be either in the ordered spin nematic (SN) state or in the disordered spin-glass (SG) state. The first phase (OG-SN) is formed under conventional cooling from normal ^{3}He. The second phase (OG-SG) is metastable, being obtained by cooling through the superfluid transition temperature, when large enough resonant continuous radio-frequency excitation is applied. NMR signature of different phases allows us to measure the parameter of the global anisotropy of the orbital glass induced by deformation.

1. Introduction. Superfluidity of ^{3}He in high porosity aerogel [1, 2] allows to investigate influence of impurities (i.e. aerogel strands) on superfluidity with nontrivial Cooper pairing. It was found that like in bulk ^{3}He two superfluid phases (called by analogy A-like and B-like) can exist in ^{3}He in aerogel in a weak magnetic field [3]. The B-like phase is analogous to bulk ^{3}He-B and has the same order parameter [3, 4]. As for the A-like phase then for many years the situation was not clear. It was proposed that the A-like phase in aerogel is described by the Larkin-Imry-Ma [5, 6] (LIM) model [7]. The random orientations of silicon strands induces spatially random distribution of ^{3}He-A order parameter. However, properties of nuclear magnetic resonance (NMR) in various aerogel samples were different and did not correspond to the properties of the fully randomized bulk A phase. Situation became much more clear when it was realized that even weak anisotropy of aerogel can influence the NMR properties and was found experimentally that in squeezed by ∼1% aerogel the A-like phase behaves as the bulk ^{3}He-A but with the orbital vector $\hat{\mathbf{l}}$ fixed along the deformation axis [8]. This observation was in agreement with LIM model developed for the case of nonzero global anisotropy [9]. It was also found that intrinsic anisotropy in some samples can be large enough to orient $\hat{\mathbf{l}}$ and all NMR properties of the A-like phase in such samples correspond to the bulk A phase order parameter oriented along some fixed axis [10].

Here we consider consequences of the theory developed in [7, 9] for different values and types of global anisotropy and report results of detailed NMR investigations of A-like phase in three aerogel samples with different anisotropy.

2. Theory. In superfluid ^{3}He, the spin-orbit interaction is small compared to other characteristic energy scales. That is why the superfluid phases of ^{3}He consist of two nearly independent subsystems of orbital and spin degrees of freedom. The bulk ^{3}He-A is characterized by nematic ordering in the spin subsystem [11] and by the ferromagnetic ordering in the orbital subsystem. Its order parameter is the matrix

$$A_{\alpha j} = \Delta \hat{d}_\alpha (\hat{e}^1_j + i\hat{e}^2_j). \qquad (1)$$

Here $\hat{\mathbf{d}}$ is unit vector describing the nematic spin order. Orthogonal unit vectors $\hat{\mathbf{e}}^1$ and $\hat{\mathbf{e}}^2$ describe orbital ferromagnetism with ferromagnetic moment along the unit vector $\hat{\mathbf{l}} = \hat{\mathbf{e}}^1 \times \hat{\mathbf{e}}^2$.

Depending on value and type of anisotropy several possible structures of the order parameter (1) can be realized in the A-like phase of ^{3}He in aerogel. For isotropic aerogel, the orbital vector $\hat{\mathbf{l}}$ is randomized due to the quenched local anisotropy provided by random orientations of aerogel strands [7]:

$$\left\langle \hat{\mathbf{l}} \right\rangle = 0, \quad \langle l_x^2 \rangle = \langle l_y^2 \rangle = \langle l_z^2 \rangle = 1/3. \qquad (2)$$

This glass state is the realization of the LIM phenomenon in ^{3}He-A. In this state the space average of the order parameter (1) is zero, $\langle A_{\alpha j} \rangle = 0$, and

$$\langle A_{\alpha i} A_{\beta j} \rangle = 0,$$
$$\langle A_{\alpha i} A^*_{\beta j} \rangle + \text{c.c.} = \frac{2}{3}\Delta^2 \delta_{ij} \left(\delta_{\alpha\beta} - \hat{h}_\alpha \hat{h}_\beta \right). \quad (3)$$

Here $\hat{\mathbf{h}}$ is unit vector along magnetic field $\mathbf{H}$ which keeps $\hat{\mathbf{d}}$ in the plane normal to $\hat{\mathbf{h}}$, where $\hat{\mathbf{d}}$ is randomized due to spin-orbit interaction with chaotic orbital momentum $\hat{\mathbf{l}}$. We call this configuration the OG-SG state, since it is the combination of the orbital glass (OG) and spin-nematic glass (SG). The OG-SG states produced by random anisotropy of aerogel strands provide the experimental realization of the random anisotropy glasses discussed in different systems [12], such as random anisotropy Heisenberg spin glasses in magnets [13, 14] and nematic glasses in liquid crystals [15–17].

Uniaxial deformation adds more states of superfluid ^{3}He-A in aerogel. Chaotic spatial distribution of the orbital vector $\hat{\mathbf{l}}$ is modified under deformation and becomes anisotropic. For squeezing or stretching of aerogel we obtain the orbital glass states with global anisotropy:

$$\left\langle \hat{\mathbf{l}} \right\rangle = 0, \quad \langle l_z^2 \rangle = \frac{1+2q}{3}, \quad \langle l_x^2 \rangle = \langle l_y^2 \rangle = \frac{1-q}{3}. \quad (4)$$

Here the axis of deformation is $\hat{\mathbf{z}}$ and we introduce parameter q of global anisotropy, which is positive in squeezed aerogel, negative in the stretched case and $q = 0$ in isotropic aerogel.

Stretching of aerogel gives the global easy plane anisotropy with $-0.5 < q < 0$ and $0 < \langle l_z^2 \rangle < 1/3$. In the limit of large stretching, q approaches the value $q = -0.5$, where $\langle l_z^2 \rangle = 0$, i.e. $\hat{\mathbf{l}}$ is kept in $\hat{\mathbf{x}} - \hat{\mathbf{y}}$ plane and the planar LIM state is formed. This orbital glass is described by the random anisotropy XY model.

Squeezing of aerogel gives the global easy axis anisotropy with $1 > q > 0$ and $1/3 < \langle l_z^2 \rangle < 1$. However, in this state q may not reach 1, because for deformations greater than some critical value [9] the orbital ferromagnetic (OF) state should be restored. In the OF state, $\left\langle \hat{\mathbf{l}} \right\rangle \neq 0$ and is parallel to the deformation axis $\hat{\mathbf{z}}$. At large squeezing, $\langle l_z \rangle$ approaches $+1$ or -1. Properties of the OF state correspond to the bulk A phase but with $\hat{\mathbf{l}}$ fixed along the axis of deformation. Observations of such ferromagnetic state were reported in [8, 10, 18]. For the intermediate squeezing deformations, the transverse components $\langle l_x^2 \rangle$ and $\langle l_y^2 \rangle$ may be substantial and the ferromagnetic order, $\langle l_z \rangle \neq 0$, is supplemented by the glass state for l_x and l_y components.

3. NMR frequency shift. The frequency shift of transverse NMR from the Larmor value is given by [19, 20]:

$$\Delta\omega/\Delta\omega_0 = -\frac{\partial U_D}{\partial \cos\beta} =$$
$$= \frac{7\cos\beta + 1}{4}(\hat{\mathbf{l}} \times \hat{\mathbf{h}})^2 - \frac{1+\cos\beta}{2}(\hat{\mathbf{l}} \cdot \hat{\mathbf{d}} \times \hat{\mathbf{h}})^2 - \cos\beta, \quad (5)$$

$$U_D = -\frac{1}{2}\sin^2\beta + \frac{1}{4}(1+\cos\beta)^2 (\hat{\mathbf{l}} \cdot \hat{\mathbf{d}} \times \hat{\mathbf{h}})^2 -$$
$$- \left(\frac{7}{8}\cos^2\beta + \frac{1}{4}\cos\beta - \frac{1}{8}\right)(\hat{\mathbf{l}} \times \hat{\mathbf{h}})^2, \quad (6)$$

where $\Delta\omega_0 = \Omega_A^2/(2\omega)$ is maximal possible value of the shift, Ω_A is Leggett frequency, β is the tipping angle of magnetization, U_D is the normalized spin-orbit (dipole-dipole) energy averaged over fast precession of magnetization. The unit vector $\hat{\mathbf{d}}$ here is the result of averaging over fast precession, it coincides with the original spin-nematic vector $\hat{\mathbf{d}}$ only for $\beta = 0$.

In the LIM state, the dipole energy should be averaged over space. The LIM characteristic length is expected to be much smaller than the dipole length, which characterizes the spin-orbit interaction, so the NMR line should not be broadened due to inhomogeneities of $\hat{\mathbf{l}}$.

We consider the general case when $\mathbf{H}$ is tilted by an angle μ to anisotropy axis $\hat{\mathbf{z}}$:

$$\hat{\mathbf{h}} = \cos\mu\ \hat{\mathbf{z}} + \sin\mu\ \hat{\mathbf{x}}. \quad (7)$$

If the global orientation of $\hat{\mathbf{l}}$ is capable to orient $\hat{\mathbf{d}}$ (to minimize U_D) then in squeezed aerogel we get:

$$\hat{\mathbf{d}} = \sin\mu\ \hat{\mathbf{z}} - \cos\mu\ \hat{\mathbf{x}}, \quad q > 0, \quad (8)$$

and in stretched aerogel:

$$\hat{\mathbf{d}} = \hat{\mathbf{y}}, \quad q < 0. \quad (9)$$

These states in deformed aerogel combine anisotropic orbital glass (OG) and the ordered spin nematic (SN) and we denote them as anisotropic OG-SN states.

If $\hat{\mathbf{l}}$ is not able to orient $\hat{\mathbf{d}}$ then the chaotic distribution of spin vector $\hat{\mathbf{d}}$ is realized:

$$\hat{\mathbf{d}} = \cos\Phi_d\,(\sin\mu\ \hat{\mathbf{z}} - \cos\mu\ \hat{\mathbf{x}}) + \sin\Phi_d\ \hat{\mathbf{y}}, \quad (10)$$

with random Φ_d. This is an anisotropic OG-SG state – the anisotropic orbital glass accompanied by spin glass. Note that the OG and SG subsystems have different characteristic length scales.

3.1. *Anisotropic OG-SN in squeezed aerogel.* In this state the spin nematic is regular, and we should average only over the orbital glass state. In squeezed aerogel, the averaging over space of (8) gives:

$$\left\langle (\hat{\mathbf{l}} \cdot \hat{\mathbf{d}} \times \hat{\mathbf{h}})^2 \right\rangle = \langle l_y^2 \rangle = \frac{1}{2}\left(1 - \langle l_z^2 \rangle\right), \quad (11)$$

$$\left\langle (\hat{\mathbf{l}} \times \hat{\mathbf{h}})^2 \right\rangle = 1 - \langle l_z^2 \rangle + \frac{1}{2} \sin^2 \mu \left(3 \langle l_z^2 \rangle - 1 \right). \quad (12)$$

Then the NMR frequency shift is

$$\frac{\Delta\omega}{\Delta\omega_0} = q \left(-\cos\beta + \sin^2 \mu \frac{7\cos\beta + 1}{4} \right). \quad (13)$$

Equation (13) with $q \approx 1$ is applicable also for the orbital ferromagnetic (OF). Therefore NMR can not distinguish between OF and OG-SN states in squeezed aerogel with $q = 1$. The latter state may be considered as multi-domain OF state or the Ising orbital glass.

3.2. *Anisotropic OG-SN in stretched aerogel.* For stretched aerogel, from (9) we obtain:

$$\left\langle (\hat{\mathbf{l}} \cdot \hat{\mathbf{d}} \times \hat{\mathbf{h}})^2 \right\rangle = \frac{1}{2} \left(1 - \langle l_z^2 \rangle \right) + \frac{1}{2} \sin^2 \mu \left(3 \langle l_z^2 \rangle - 1 \right), \quad (14)$$

and the corresponding NMR frequency shift is

$$\frac{\Delta\omega}{\Delta\omega_0} = q \left(-\cos\beta + \sin^2 \mu \frac{5\cos\beta - 1}{4} \right). \quad (15)$$

3.3. *Anisotropic orbital glass + spin glass.* In the OG-SG state the spin-nematic vector $\hat{\mathbf{d}}$ in (10) is random, and we obtain:

$$\left\langle (\hat{\mathbf{l}} \cdot \hat{\mathbf{d}} \times \hat{\mathbf{h}})^2 \right\rangle = \frac{1}{2} \left\langle (\hat{\mathbf{l}} \times \hat{\mathbf{h}})^2 \right\rangle, \quad (16)$$

with $\left\langle (\hat{\mathbf{l}} \times \hat{\mathbf{h}})^2 \right\rangle$ from (12). Then $\Delta\omega$ is given by:

$$\frac{\Delta\omega}{\Delta\omega_0} = q \cos\beta \left(\frac{3}{2} \sin^2 \mu - 1 \right), \quad (17)$$

which is valid for both squeezed and stretched aerogel.

4. Conditions of experiments. Three different aerogel samples with porosity of 98.2% and with different types and values of anisotropy were used. All the samples had cylindrical form with axes oriented along $\hat{\mathbf{z}}$. Diameter and height of the samples (in mm) were the following: 4 and 4 (sample 1), 3.8 and 5 (sample 2), 6 and 3 (sample 3). The experimental chamber (Fig.1) was made from epoxy resin "Stycast-1266". The upper cell (1 and 2 on Fig.1) was used first for sample 1 and then for sample 2. Samples 1 and 2 had gaps ~0.1 mm from side walls of the cell but were squeezed at room temperature along $\hat{\mathbf{z}}$-axis by 8% and 3% respectively, i.e. after cooling their deformation should be 9% and 4% due to additional thermal shrinkage of epoxy walls by ~1%. Sample 3 was placed freely in the cell with the gaps ~0.1 mm from side and top walls to avoid such additional deformation. Its residual anisotropy was measured at room temperature by light birefringence [21] and was less than 0.1%.

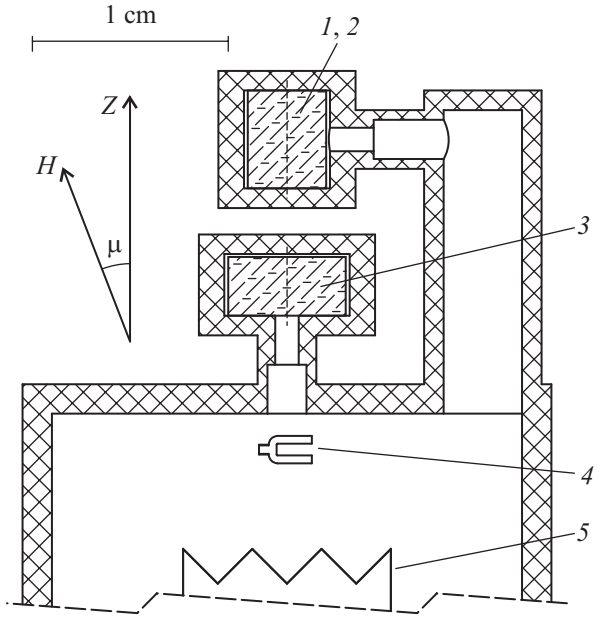

Fig.1. Sketch of experimental chamber. *1*, *2* – samples 1 or 2; *3* – sample 3; *4* – quartz tuning fork; *5* – heater

In order to avoid paramagnetic signal from solid ^{3}He, aerogel samples were preplated by ~2.5 monolayers of ^{4}He. Each sample was surrounded by transverse NMR coil (not shown in Fig.1) with the axis along $\hat{\mathbf{x}}$. We were able to rotate $\mathbf{H}$ by any angle in $\hat{\mathbf{y}} - \hat{\mathbf{z}}$ plane and also by $\pm 15^\circ$ in $\hat{\mathbf{x}} - \hat{\mathbf{y}}$ plane. Experiments were carried out in magnetic fields from 95 to 424 Oe (corresponding NMR frequencies are from 310.5 KHz to 1.38 MHz) and at pressures 26.0 (sample 1) and 27.2 bar (samples 2 and 3). Necessary temperature was obtained by nuclear demagnetization cryostat and was measured by quarz tuning fork, calibrated by Leggett frequency measurements in bulk ^{3}He-B.

5. Continuous wave NMR experiments. For sample 1 and for $\mathbf{H} \parallel \hat{\mathbf{z}}$, the continuous wave (CW) NMR shift in the A-like phase was negative as it is expected from (13) for μ=0. For 9% squeezing we should get the orbital ferromagnetic phase with $q \approx 1$, since from [8] it follows that the critical value of anisotropy is less than 1%. Therefore from the value of the shift we can extract the Leggett frequency for this sample. Temperature of superfluid transition T_{ca} of ^{3}He in aerogel is not well defined. In particular, on warming NMR shift in the B-like phase disappears at temperature by $\sim 0.02\, T_{ca}$ higher than in A-like phase [10]. Therefore, to compare our data with results of previous experiments [8, 10, 22, 23] we defined T_{ca}^* as the temperature when the temperature dependence of the NMR frequency shift in the A-like phase is extrapolated to zero. Then all the data were recalculated to the same pressure (26.0 bar)

using pressure dependence of the Leggett frequency in bulk ^{3}He-A [24]. Correction coefficients for the shift were 0.854 (for 29.3 bar), 0.881 (28.6 bar), 0.949 (27.2 bar) and 1.066 (for 25 bar). Fig.2 shows the resulting

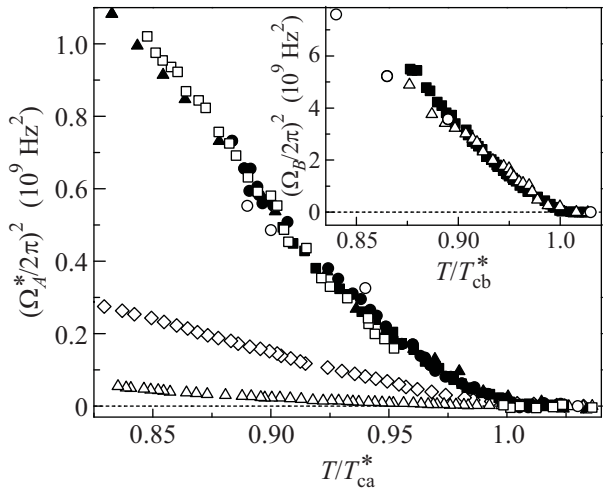

Fig.2. Temperature dependence of the "effective" Leggett frequency in the A-like phase and Ω_B in B-like phase (insert) in different aerogel samples rescaled to 26 bar pressure. (□) – sample 1 (9% squeezing, 26.0 bar); (▲) – squeezed by 4% aerogel (29.3 bar) [8]; (●) – intrinsically anisotropic aerogel (28.6 bar) [22]; (■) – intrinsically anisotropic aerogel (26.0 bar) [10]; (○) – aerogel squeezed radially by 20% (25.0 bar) [23]; (◇) – sample 2 (27.2 bar); (△) – sample 3 (27.2 bar)

"effective" Leggett frequency $(\Omega_A^*)^2 = 2\omega|\Delta\omega|$ obtained in these CW NMR experiments ($\beta = 0$). It is seen that all the data (except for samples 2 and 3) collapse into the same curve. This suggests that the orbital ferromagnetic state with $q \approx 1$ was obtained in these experiments. Correspondingly the obtained $\Omega_A^*(T)$ is in fact the true Leggett frequency $\Omega_A(T)$. The values of T_{ca}^* for our samples were found to be $0.74T_c$ (sample 1, 26.0 bar), $0.722T_c$ (sample 2, 27.2 bar), $0.77T_c$ (sample 3, 27.2 bar), where T_c is the superfluid transition temperature of the bulk ^{3}He.

Measurements of the Leggett frequency in the B-like phase (Ω_B) were also done with sample 3 using a prominent kink at the low field region of the CW NMR line. The results were compared with the B-like phase data published in [10, 23]. Here we also have recalculated the data to pressure of 26 bar using pressure dependence of the Leggett frequency in B-like phase measured in [25] (correction coefficients were 1.026 for 25 bar and 0.983 for 27.2 bar). It is seen that these data also collapse to a single curve (insert in Fig.2) if we define $T_{cb}^* \approx T_{ca}$ as the temperature when the frequency shift in the B-like phase is extrapolated to zero.

In contrast to sample 1, frequency shifts in samples 2 and 3 for $\mathbf{H} \parallel \hat{\mathbf{z}}$ were much smaller and positive (see Fig.2 and the mainframe Fig.3). It can be explained if

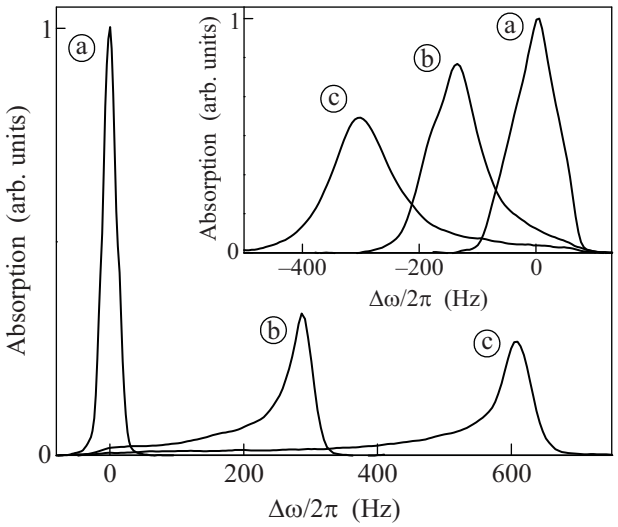

Fig.3. NMR absorption lines in sample 2 in the OG-SN state (orbital glass combined with regular spin nematic) for $\mathbf{H} \parallel \hat{\mathbf{z}}$. NMR frequency is 328.5 kHz. a – $T > T_{ca}^*$; b – $T = 0.88\,T_{ca}^*$; c – $T = 0.77\,T_{ca}^*$. Insert: NMR lines in the OG-SG state (orbital glass accompanied by spin glass) for $\mu = 90^\circ$ at corresponding conditions

we suggest that in both cases we have stretched aerogel with the anisotropic OG-SN state, i.e. the orbital glass combined with regular spin nematic. Rotation of $\mathbf{H}$ in $\hat{\mathbf{x}} - \hat{\mathbf{y}}$ plane did not change NMR properties, i.e. the observed state is nearly isotropic in this plane.

We assume that in both samples the Leggett frequency equals to the value which follows from the most of the data in Fig.2. Then from the measured values of $\Delta\omega$ we obtain that $q \approx -0.25$ for sample 2 and $q \approx -0.05$ for sample 3, i.e. the sample 3 is close to isotropic aerogel. The fact that sample 2 was squeezed by ~4% but behaves like stretched sample can be explained by large initial intrinsic stretching: this sample was grown in quartz tube with i.d. of 4 mm, but for unknown reason it was shrunk in diameter by about 5-6% after preparation.

To confirm that in samples 2 and 3 we have stretched aerogel with the orbital glass state, we have measured CW NMR shifts for different angles μ between $\hat{\mathbf{z}}$ and $\mathbf{H}$. For the anisotropic OG-SN state in stretched aerogel (see (15)) and for CW NMR ($\cos\beta$=1) we get

$$\Delta\omega = A\cos^2\mu, \qquad (18)$$

where $A = -q\Delta\omega_0$. Note that for stretched aerogel one has q <0, i.e. $\Delta\omega$ is always positive. The obtained dependence of $\Delta\omega$ versus μ for sample 2 is shown in Fig.4

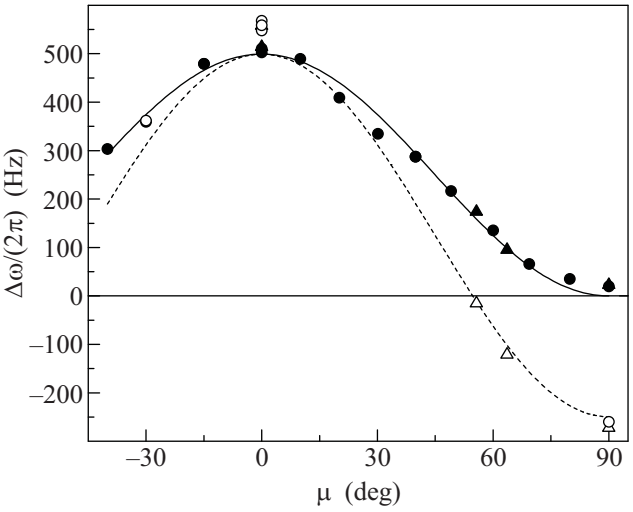

Fig.4. Dependence of CW NMR frequency shift in the A-like phase (sample 2) on the angle μ between sample axis and $\mathbf{H}$. Filled symbols were obtained after cooling through T_{ca} with low RF field and open symbols – with high RF excitation. NMR frequency is 328.5 KHz, but data shown by triangles were obtained at 341.5 KHz and were rescaled to 328.5 KHz. Solid line is the best fit of filled symbols by (18), while the dashed line is the theoretical dependence (17). $T = 0.81\,T^*_{ca}$

by filled symbols. Solid line is the best fit by theoretical dependence (18) with A=499 Hz. It gives us the same $q = -0.25$ for this sample as obtained from Fig.2.

The orbital glass with the limiting value $q = -0.5$ was first introduced in [23]. This planar LIM state of ^{3}He-A was suggested to explain the NMR experiments in aerogel obtained by 20% radial squeezing of cylindrical sample, which would correspond to a large stretching deformation needed to form the XY orbital glass. The identification was based on the comparison of the measured NMR frequency shifts in A- and B-like phases which was found to be about twice less than in bulk ^{3}He. However, according to Fig.2, the value of Ω^*_A obtained in [23] more likely corresponds to the orbital ferromagnetic state, rather than to the planar LIM state. In principle, a small inhomogeneity in radial deformation can destroy the planar LIM state in the most parts of the sample and restore the ferromagnetic order with the anisotropy axis laying in the $\hat{\mathbf{x}} - \hat{\mathbf{y}}$ plane. As for the ratio of Ω^2_A/Ω^2_B then it seems that in ^{3}He in aerogel it is less than in bulk superfluid (see Fig.2).

The data described above were obtained if low level of radio-frequency (RF) excitation was used to monitor the NMR line on cooling through T_{ca}. Earlier it was found [26, 22] that the A-like phase may exist in two states. One state is obtained if on cooling through T_{ca} the low level of RF (or no RF) is used. Another one is created by violent perturbation of the spin system during cooling: when cooling through T_{ca} is accompanied either by a very high CW RF excitation (which saturates NMR signal in normal phase) or by large tipping pulses. We suggest that in this case the OG-SG state (the orbital glass combined with the spin glass) can be created. The point is that saturation of the NMR line just below T_{ca} (where the dipole energy is small) results in fast rotation of $\hat{\mathbf{d}}$. Further cooling can "freeze" the chaotic distribution of $\hat{\mathbf{d}}$ in the plane normal to $\mathbf{H}$.

To check this possibility we carried out "high RF cooling through T_{ca}" experiments with samples 2 and 3. The CW RF field was kept ~0.015 Oe which is about 50 times larger than usual, so that the NMR line in normal phase was fully saturated. After cooling below $\sim 0.9\,T_{ca}$, the RF level was reduced to its normal value. NMR lines obtained in such experiment for $\mu = 90^\circ$ are shown in the insert to Fig.3. It was found that the state which appears after such cooling well corresponds to the OG-SG state in stretched aerogel. By open symbols in Fig.4 are shown results obtained in the OG-SG state in sample 2 in CW NMR. This can be compared with the filled symbols obtained for the spin-nematic state (OG-SN) in the same sample at the same conditions. Dashed curve is the theoretical dependence expected for spin glass, $\Delta\omega = -A\left(\frac{3}{2}\sin^2\mu - 1\right)$ (see Eq. (17) for $\cos\beta$=1). There are no fitting parameters here because the prefactor A is already found to be 499 Hz at this temperature from measurements on the OG-SN state. There is a small discrepancy between theory and experiment for $\mu = 0$. This may occur if the characteristic length of the spin glass is comparable with the dipole length. Then an additional shift connected with the gradient energy of the $\hat{\mathbf{d}}$-field distribution appears.

In conclusion to this section we should mention that similar dependencies as shown in Fig.4 were obtained in sample 3 but values of the shifts were smaller in accordance to the smaller value of q in this sample. The width of the NMR line in sample 3 was of the order of the shift, i.e. stretching of this sample seems to be inhomogeneous. It means that the obtained value of q is in fact the value averaged over the sample volume.

6. Pulsed NMR experiments. Samples 2 and 3 were also investigated by pulsed NMR. Below we present the results of experiments with sample 2 which were more systematic, but we should mention that results for sample 3 were similar.

From (15) and (17) we can obtain dependencies for $\Delta\omega$ on β for different orientations of $\mathbf{H}$. The remarkable feature of (15) and (17) is that we can introduce the critical angle μ_c. If $\mu < \mu_c$ then the frequency of

free induction decay signal (FIDS) should decrease with β in range $0 < \beta < 180°$, while for $\mu > \mu_c$ the frequency should grow with increase of β. For $\mu = \mu_c$ no dependence of FIDS frequency on β is expected. The value of μ_c is different for the OG-SN and OG-SG states (the states with oriented and disordered spin nematic vector respectrively). In the OG-SN state, from (15) we get that $\sin^2\mu_c = 4/5$ (i.e. $\mu_c \approx 63.4°$), while for the OG-SG state from (17) we get $\sin^2\mu_c = 2/3$ and $\mu_c \approx 54.7°$.

After application of single RF tipping pulse the FIDS was amplified and then recoded by digital oscilloscope. In order to determine FIDS frequency for a given β, the obtained time dependence of the frequency was extrapolated to the initial moment. The RF pulse was short (15 periods at frequency ~300 KHz), so its spectral width was large enough. The measured dependencies $\Delta\omega(\beta)$ for different μ are shown in Fig.5 for OG-SN state and

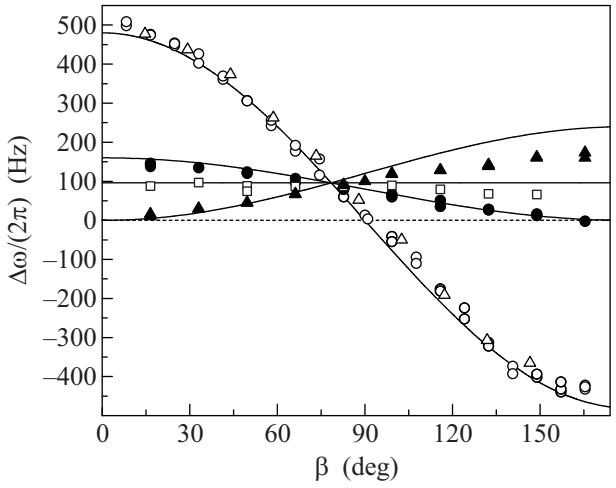

Fig.5. Frequency of FIDS in the A-like phase (sample 2) versus β for different μ in case when low RF excitation was used while cooling through T_{ca}. (○) and (△) - $\mu = 0$; (●) - $\mu = 54.7°$; (□) - $\mu = \mu_c = 63.4°$; (▲) - $\mu = 90°$. Solid lines are theoretical curves for corresponding μ with no fitting parameters. NMR frequency is 341.5 KHz (except △, which were obtaned at 664 KHz but rescaled to 341.5 KHz). $T = 0.81\,T^*_{ca}$

in Fig.6 for OG-SG state. In both figures the theoretical functions $\Delta\omega(\beta)$ for corresponding values of μ are drawn by solid lines. No fitting parameters were used for these lines. The parameter $A = -q\Delta\omega_0$=480 Hz was obtained from its value found in CW measurements (A=499 Hz) after rescaling to the frequency 341.5 KHz.

It is seen that deviations from theoretical curves in Fig.5 are small. These deviations are more prominent at large tipping angles that can be due to inhomogeneity of RF field which was estimated to be about 15%.

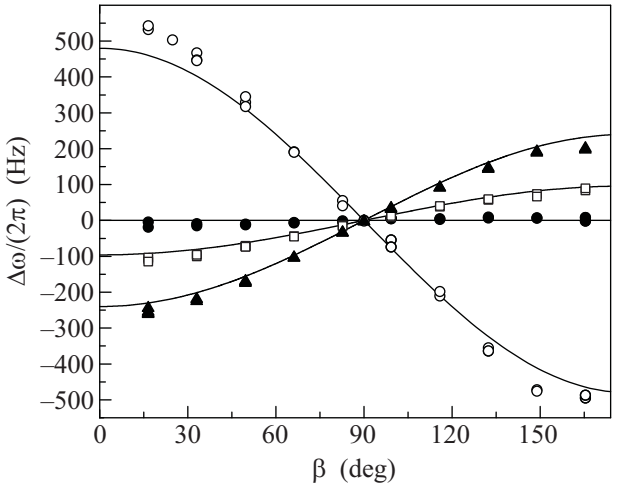

Fig.6. Frequency of FIDS in the A-like phase (sample 2) versus β for different μ in case when very high RF excitation was used while cooling through T_{ca}. (○) - $\mu = 0$; (●) - $\mu = \mu_c = 54.7°$; (□) - $\mu = 63.4°$; (▲) - $\mu = 90°$. Solid lines are theoretical curves for corresponding μ with no fitting parameters. NMR frequency is 341.5 KHz, $T = 0.81\,T^*_{ca}$

Deviations in Fig.6 for μ=0 and small β are clearly due to the same reason as in CW NMR (see Fig.4).

7. Discussion. Two states of ^{3}He-A in aerogel have been discussed here, OG-SN and OG-SG. Both represent orbital glass (OG) – the anisotropic glass state of the orbital vector $\hat{\mathbf{l}}$. They differ by the structure of the spin subsystem, which is either in the spin nematic (SN) phase or in the disordered spin-glass (SG) state. The OG-SG state was obtained by cooling through T_c when a large resonant CW RF excitation was applied, while the OG-SN phase is formed under conventional cooling through T_c. We observe both these states in each of two stretched aerogel samples: with small and large deformations.

Leggett frequency in A-like phase of ^{3}He in 98.2% aerogel was measured using squeezed sample. The results are in a good agreement with previous data. This suggests that the Leggett frequency is nearly the same for all samples and allows to estimate the deformation parameter q for stretched aerogel samples, which characterizes the uniaxial global anisotropy of orbital glass.

Most of the previous NMR results in A-like phase can be explained in frames of the Larkin-Imry-Ma random anisotropy model. In particular, "soliton-like" spin state observed in [22] corresponds to the orbital ferromagnetic state accompanied by the spin glass state (OF-SG). It is also now clear that aerogel samples can be intrinsically stretched. It is possible that in some samples we have both stretched and squeezed regions. Such situation is more probable in weakly anisotropic

samples. It is also possible that some samples have bi-axial global anisotropy with $\langle l_x^2\rangle \neq \langle l_y^2\rangle \neq \langle l_z^2\rangle$. Then we can obtain other than (13), (15) or (17) dependencies for $\Delta\omega$ on β. For example, in the bi-axial OG-SN state with $\langle l_z^2\rangle \approx 1/3$, and $\langle l_x^2\rangle \neq \langle l_y^2\rangle$ for μ=0 one gets $\Delta\omega \propto (1+\cos\beta)$. Such dependence was observed in weakly anisotropic aerogel samples in [27, 26, 10].

We conclude that the LIM model for the orbital glass state of the A-like phase is in a good agreement with the most of experimental data. Correspondingly the model of "robust" superfluid phase for the A-like phase suggested in [28] is not realized in practice at least for values of anisotropy $\geq$0.1%. However, many questions concerning the superfluid ^{3}He in aerogel still remain. For example, it is not clear why the NMR frequency shift in the B-like phase disappears at temperature higher than in the A-like phase, and why the ratio of Leggett frequencies in the A-like and B-like phases at the same conditions is less than the same ratio for bulk A and B phases. The first phenomenon may occur because q can depend on temperature (at least near T_{ca}).

It is also not known how q is related to the magnitude of deformation. The transition from the orbital glass to the orbital ferromagnetic state was not yet observed and the value of critical anisotropy has not been measured. This is the subject of further investigations.

This work was supported in part by RFBR grants (# 09-02-01185 and # 09-02-12131ofi) and by the Academy of Finland, Centers of excellence program 2006-2011. It is a pleasure to thank E. Kats for helpful comments.

1. J. V. Porto and J. M. Parpia, Phys. Rev. Lett. **74**, 4667 (1995).
2. D. T. Sprague, T. M. Haard, J. B. Kycia et al., Phys. Rev. Lett. **75**, 661 (1995).
3. B. I. Barker, Y. Lee, L. Polukhina et al., Phys. Rev. Lett. **85**, 2148 (2000).
4. V. V. Dmitriev, V. V. Zavjalov, I. V. Kosarev et al., Pis'ma v ZhETF **76**, 371 (2002) [JETP Lett. **76**, 321 (2002)].
5. A. I. Larkin, ZhETF **58**, 1466 (1970) [JETP **31**, 784 (1970)].
6. Y. Imry and S. K. Ma, Phys. Rev. Lett. **35**, 1399 (1975).
7. G. E. Volovik, Pis'ma v ZhETF **63**, 281 (1996) [JETP Lett. **63**, 301 (1996)]; Pis'ma v ZhETF **84**, 533 (2006) [JETP Lett. **84**, 455 (2006)].
8. T. Kunimatsu, T. Sato, K. Izumina et al., Pis'ma v ZhETF **86**, 244 (2007) [JETP Lett. **86**, 216 (2007)].
9. G. E. Volovik, J. of Low Temp. Phys. **150**, 453 (2008).
10. V. V. Dmitriev, D. A. Krasnikhin, N. Mulders et al., Pis'ma v ZhETF **86**, 681 (2007) [JETP Lett. **86**, 594 (2007)].
11. A. F. Andreev and I. A. Grishchuk, ZhETF **87**, 467 (1984) [Sov. Phys. JETP **60**, 267 (1984)].
12. A. A. Fedorenko and F. Kühnel, Phys. Rev. B **75**, 174206 (2007).
13. M. Itakura, Phys. Rev. B **68**, 100405 (2003).
14. V. Dotsenko, arXiv:1001.3023.
15. E. I. Kats, Pis'ma v ZhETF **65**, 695 (1997) [JETP Lett. **65**, 725 (1997)].
16. D. E. Feldman and R. A. Pelcovits, Phys. Rev. E **70**, 040702(R) (2004).
17. G. Feio, J. L. Figueirinhas, A. R. Tajbakhsh, and E. M. Terentjev, Phys. Rev. B **78**, 020201(R) (2008).
18. T. Sato, T. Kunimatsu, K. Izumina et al., Phys. Rev. Lett. **101**, 055301 (2008).
19. A. D. Gongadze, G. E. Gurgenishvili, and G. A. Kharadze, ZhETF **78**, 615 (1980) [Sov. Phys. JETP **51**, 310 (1980)].
20. Yu. M. Bunkov and G. E. Volovik, Europhys. Lett. **21**, 837 (1993).
21. P. Bhupathi, J. Hwang, R. M. Martin et al., Optics Express **17**, 10599 (2009).
22. V. V. Dmitriev, D. A. Krasnikhin, N. Mulders, and D.E. Zmeev, J. of Low Temp. Phys. **150**, 493 (2008).
23. J. Elbs, Yu. M. Bunkov, E. Collin et al., Phys. Rev. Lett. **100**, 215304 (2008).
24. A. I. Ahonen, M. Krusius, and M.A. Paalanen, J. of Low Temp. Phys. **25**, 421 (1976).
25. V. V. Dmitriev, N. Mulders, V. V. Zavjalov, and D. E. Zmeev, AIP Conf. Proc. **850**, 229 (2006).
26. V. V. Dmitriev, L. V. Levitin, N. Mulders, and D. E. Zmeev, Pis'ma v ZhETF **84**, 539 (2006) [JETP Lett. **84**, 461 (2006)].
27. O. Ishikawa, R. Kado, H. Nakagawa et al., AIP Conf. Proc. **850**, 235 (2006).
28. I. A. Fomin, ZhETF **125**, 1115 (2004) [JETP **98**, 974 (2004)].